

# Using a microfluidic device for 1 $\mu$ l DNA microarray hybridization in 500 s

Cheng-Wey Wei<sup>1,2</sup>, Ji-Yen Cheng<sup>1,\*</sup>, Chih-Ting Huang<sup>1</sup>, Meng-Hua Yen<sup>1,2</sup> and Tai-Horng Young<sup>2</sup>

<sup>1</sup>Research Center for Applied Sciences, Academia Sinica, Taipei 11529, Taiwan and <sup>2</sup>Institute of Biomedical Engineering, National Taiwan University, Taipei 10051, Taiwan

Received December 17, 2004; Revised March 25, 2005; Accepted April 20, 2005

## ABSTRACT

This work describes a novel and simple modification of the current microarray format. It reduces the sample/reagent volume to 1  $\mu$ l and the hybridization time to 500 s. Both 20mer and 80mer oligonucleotide probes and singly labeled 20mer and 80mer targets, representative of the T-cell acute lymphocytic leukemia 1 (TAL1) gene, have been used to elucidate the performance of this hybridization approach. In this format, called shuttle hybridization, a conventional flat glass DNA microarray is integrated with a PMMA microfluidic chip to reduce the sample and reagent consumption to 1/100 of that associated with the conventional format. A serpentine microtrench is designed and fabricated on a PMMA chip using a widely available CO<sub>2</sub> laser scribe. The trench spacing is compatible with the inter-spot distance in standard microarrays. The microtrench chip and microarray chip are easily aligned and assembled manually so that the microarray is integrated with a microfluidic channel. Discrete sample plugs are employed in the microchannel for hybridization. Flowing through the microchannel with alternating depths and widths scrambles continuous sample plug into discrete short plugs. These plugs are shuttled back and forth along the channel, sweeping over microarray probes while re-circulation mixing occurs inside the plugs. Integrating the microarrays into the microfluidic channel reduces the DNA–DNA hybridization time from 18 h to 500 s. Additionally, the enhancement of DNA hybridization reaction by the microfluidic device is investigated by determining the coefficient of variation (CV), the growth rate of the hybridization signal and the ability to discriminate single-base

mismatch. Detection limit of 19 amol was obtained for shuttle hybridization. A 1  $\mu$ l target was used to hybridize with an array that can hold 5000 probes.

## INTRODUCTION

The DNA microarray is a highly effective approach for high-throughput gene expression analysis and genotyping. Target DNA molecules suspended in the solution can pair with surface-bound DNA probes through heterogeneous DNA–DNA hybridization to determine simultaneously the relative concentration of multiple targets in the sample.

Microarray analysis has become a powerful technology for drug screening, disease gene identification and signaling pathway studies. However, one of the serious limitations on the reaction of biomolecules is the slow diffusion kinetics. For instance, in a DNA–DNA hybridization experiment, the pairing reaction normally takes >12 h (overnight) to run to completion (1,2). Furthermore, the sample and reagent volumes required for conventional DNA–DNA hybridization reaction are quite large. A 100  $\mu$ l sample is usually consumed for a 25  $\times$  75 mm<sup>2</sup> slide (3) that bears 10 000 probes. The large amount required sometimes constrains the practical application of the powerful DNA microarray.

Thermodynamic equilibrium is critical in heterogeneous DNA hybridization assay. Considerable cross-hybridization occurs under non-equilibrium conditions (4). Furthermore, a lower target concentration corresponds to a longer equilibrium time. Genes that are down-regulated require longer times to be measured with the same accuracy as those that are up-regulated (4,5). For optimized probes for which cross-hybridization is very low, the time taken to reach equilibrium still depends on target concentration. Therefore, systematic hybridization bias is frequently found when the hybridization reaction is not driven to completion.

\*To whom correspondence should be addressed at 128 Sec. 2 Academia Road, Taipei 11529, Taiwan. Tel: +886 2 2789 8000; Fax: +886 2 2782 6680; Email: jycheng@gate.sinica.edu.tw

The diffusion constant of DNA in water is extremely low ( $D_w = 4.9 \times 10^{-9} \text{ cm}^2/\text{s} \times [\text{bp}]^{-0.72}$ ,  $D_w = 2.1 \times 10^{-7} \text{ cm}^2/\text{s}$  for 80mer) (6), so the equilibrium result is obtained after 12–15 h at a concentration of  $10^{-13}$  to  $10^{-14}$  M (corresponding to  $10^6$  to  $10^7$  target copies per 100  $\mu\text{l}$  of target solution). Hence, DNA microarray hybridization is typically performed overnight to ensure that the reaction runs to completion. Although in some hybridization stations convection motion is used to enhance hybridization, the effect is not significant. Some researchers have found that 66 h is needed for complete hybridization so that the microarray result can be significantly improved (5). Accelerating the reaction is advantageous.

Even when the reaction is performed overnight, not all of the target molecules can react with all of the surface-bound probes. For example, for 80mer target DNA in water, the corresponding diffusion length [ $l = \sqrt{2Dt}$ , where  $D$  is the diffusion constant and  $t$  is the diffusion time (7)] is 1.9 mm for one day. Restated, each probe has the opportunity to react only with nearby targets and the complementary targets that are outside the diffusion range are wasted. Normally, a 10 000-probe array is 20 mm  $\times$  30 mm. The sample utilization efficiency is quite low under the diffusion process. Only  $\sim 0.3\%$  of the target in the sample is consumed.

The current DNA microarray experiment consumes  $\sim 10 \mu\text{g}$  total RNA for a  $\sim 10$  000 probe microarray (1,8,9). The amount corresponds to  $\sim 2.5 \times 10^7$  cells. The sample consumption can be greatly reduced by increasing the hybridization efficiency. If both the reaction time and the sample consumption are reduced, then the application of the DNA microarray can be further expanded. For instance, low copy genes can be analyzed more accurately. Genotyping by microarray may be performed without amplifying the sample. Many strategies have been proposed to enhance the hybridization efficiency and reduce the hybridization time.

Cheek *et al.* (10) employed a flow-through 3D microchannel chip combined with chemiluminescence detection to reduce the signal variation and the detection limit. The authors achieved signal SD of 8.1% and a detection limit of 250 amol. The hybridization time was 3 h. The targets were 19mer to 34mer short oligonucleotides.

Adey *et al.* (11) presented a unique microfluidic device that used pneumatically powered pumps for active mixing in a 25  $\mu\text{m}$ -thick chamber to increase sensitivity by a factor of 2–3. An air compressor generated a vacuum source and was used in the pneumatic system. A 35  $\mu\text{l}$  sample was hybridized overnight in the device. The target was multiply labeled with Cy3- or Cy5- dCTP by PCR. A target quantity as low as 9.4 amol was detected.

Liu and Rauch (12) used a special substrate surface combined with a microfluidic channel device to reduce the reaction time. The device exploited passive mixing by sample oscillation in a filled microfluidic channel to reduce the reaction time. A 200  $\mu\text{l}$  of 41mer oligonucleotide is used in the hybridization. A 1 fmol target was detected on the special surface in 15 min.

Soper and co-workers (13) used a PMMA microfluidic device assembled with a low-density array to reduce the hybridization time. In their study, four oligonucleotide probes (21mer) with an inter-spot diameter of 400  $\mu\text{m}$  were printed into a PMMA microfluidic channel. A hybridization signal with an S/N ratio of two was obtained with 10 pM 21mer targets labeled with infrared dye.

The authors also attempted to reduce the amount of sample consumed by integrating microfluidic channels into a DNA microarray, using widely available  $\text{CO}_2$  laser micromachining (14).

Li and co-workers (15) modeled the microarray hybridization kinetics of a microfluidic device. Reducing the channel height reduces the time required to reach a steady state. This effect is caused by the faster convection near the surface in the smaller channels. Hybridization in the microchannel indeed reduces the reaction time. A continuous flow of the hybridization solution is used in the modeling. However, the modeling for hybridization in discrete droplets (or plugs) has not yet been investigated.

Although reducing the dimensions of the microchannels reduces the diffusion length, a low Reynolds number for the microfluidic channel is known to cause a laminar flow that hinders effective mixing. The microchannel hybridization that employs the filled continuous sample flow involves this problem. Various measures have been developed to improve the mixing inside the channel.

Yaralioglu *et al.* (16) applied on-chip ultrasonic transducers to cause active mixing around the transducers. The primary mixing mechanism is acoustic streaming. Mixing occurs near the region of the transducer.

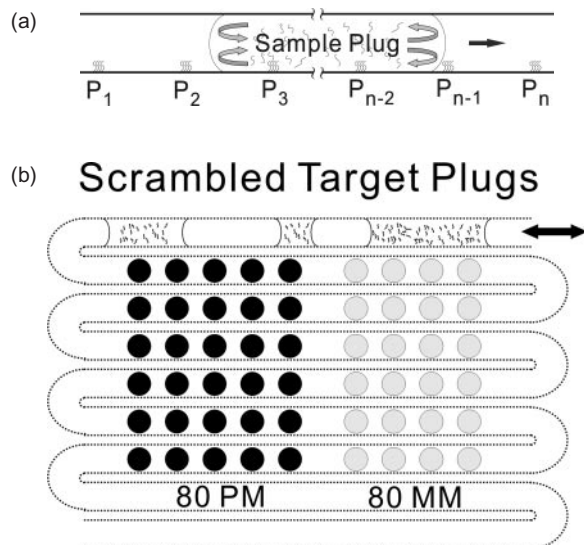
Stroock *et al.* (17) demonstrated passive mixing by chaotic advection. The mixing is caused by chevron ridges embossed on the bottom of the channel. This method strategy has been demonstrated mainly for continuous liquid flow.

Chaotic advection mixing in the microchannel has also been used to mix viscous aqueous droplets efficiently (18). When reagents are localized within the discrete droplet in a microchannel with a low Reynolds number, they can be mixed quickly by re-circulating flows caused by the shearing interaction of the fluid in the plug with the walls of the microchannel (19–21). Mixing is further promoted using winding channels (22). Such mixing does not depend on special architecture on the channel wall. Additionally, the volume can be reduced by using a discrete plug rather than a continuous sample flow.

None of the aforementioned hybridization efficiency improvements simultaneously exhibits all of the following characteristics:

- (i) Compatibility with widely used flat glass slide DNA microarray format.
- (ii) Compatibility with extensively used Cy3/Cy5 fluorescence scanners.
- (iii) Reduction of hybridization time from overnight to several minutes.
- (iv) Reduction of sample and reagent consumption to 1  $\mu\text{l}$  (corresponding to total RNA quantity of  $\sim 0.5 \mu\text{g}$ ).
- (v) Reduction of signal bias among of high-copy and low-copy transcripts (4).
- (vi) Omission of need for complex automation system, and capacity to be operated manually or automatically.

A new strategy that integrates microfluidic channels with microarrays to overcome the conventional microarray's shortcomings is needed. In this work, an effort is made to utilize chaotic mixing of droplets to enhance the hybridization efficiency and reduce the hybridization time. A simple device was fabricated to integrate a DNA microarray with microfluidic



**Scheme 1.** (a) Droplet shuttle hybridization in microchannel.  $P_1, P_2, \dots, P_n$  refer to the probe spots. The black arrow indicates the direction of liquid plug flow and the gray arrows denote the direction of the re-circulating flow inside the plug. The liquid/air interface show slightly concave shape because of the hydrophilic wall surface. (b) An illustration showing that scrambled discrete plugs sweep over different probes in the channel. This example shows thirty PM probe spots and twenty-four MM probe spots.

channel (Scheme 1). A sample solution is introduced into the microchannel and scrambled into discrete plugs to induce droplet mixing. The discrete plugs are then shuttled through the entire microchannel (shuttle hybridization), sweeping over DNA probes to perform hybridization, as indicated by the cross-sectional view in Scheme 1a. During shuttling, the plugs are thoroughly mixed by the natural re-circulating flows. Notably, the target solution does not entirely fill the channel so that sample amount is reduced. A 5'-terminal singly labeled synthetic oligonucleotide is used as the target in this work to simplify the data analysis. The sequence of the gene T-cell acute lymphocytic leukemia 1 (TAL1) is used. The length of the DNA is the practical limit for the synthetic oligonucleotide that can be commercially obtained. The enhancement on single-base discrimination ability with this shuttle hybridization is also investigated.

## MATERIALS AND METHODS

Synthetic 5'-biotin-labeled oligonucleotides are acquired from MWG (Germany). Table 1 presents the TAL1 probe and the target sequences. The microarray slides are home-prepared aminosilane-treated sodalime slides (Kimble) or commercial aminated slides (CORNING UltraGAPS Coated Slides). The thickness of the slides is 1 mm.

### Fabricating microfluidic chip

The authors' previous work reported the fabrication of microfluidic chips (23). Briefly, a commercial CO<sub>2</sub> laser scriber (M-300, Universal Laser Systems, USA) is used to engrave the PMMA substrate to fabricate a microtrench. The microtrench pattern is designed using CorelDraw (Corel) and then

**Table 1.** TAL1 probe and target sequences of the oligonucleotides used in the hybridization experiments

Name	Sequence (5'→3')
80 PM (TAL1)	AAGAGGAGACCTTCCCCCTATGAGATGG AGATTACTGATGGTCCCCACACCAAAG TTGTGCGGCGTATCTTACCAA
80 MM	TGCTGGAGTGAGATATTAATAAAAAACAGG CTGGACTGATGGTCCCCACACACCAGT TGCCCATGACTGGGGTACTACA
80 Target (TAL1)	TTGGTGAAGATACGCCGACAACCTTTTGG TGTGGGGGACCATCAGTAATCTCCATCTCA TAGGGGGGAAGGTCTCCTCTT
PM	GATTCAATGCCTCTGGCTCT
MM1	AATTC AATGCCTCTGGCTCT
MM2	GATTTAATGCCTCTGGCTCT
MM3	GATTC AATGTCTCTGGCTCT
MM4	GATTC AATGCTCTAGCTCT
MM5	GATTC AATGCCTCTGGCTCC
Target	AGAGCCAGAGGCATTGAATC

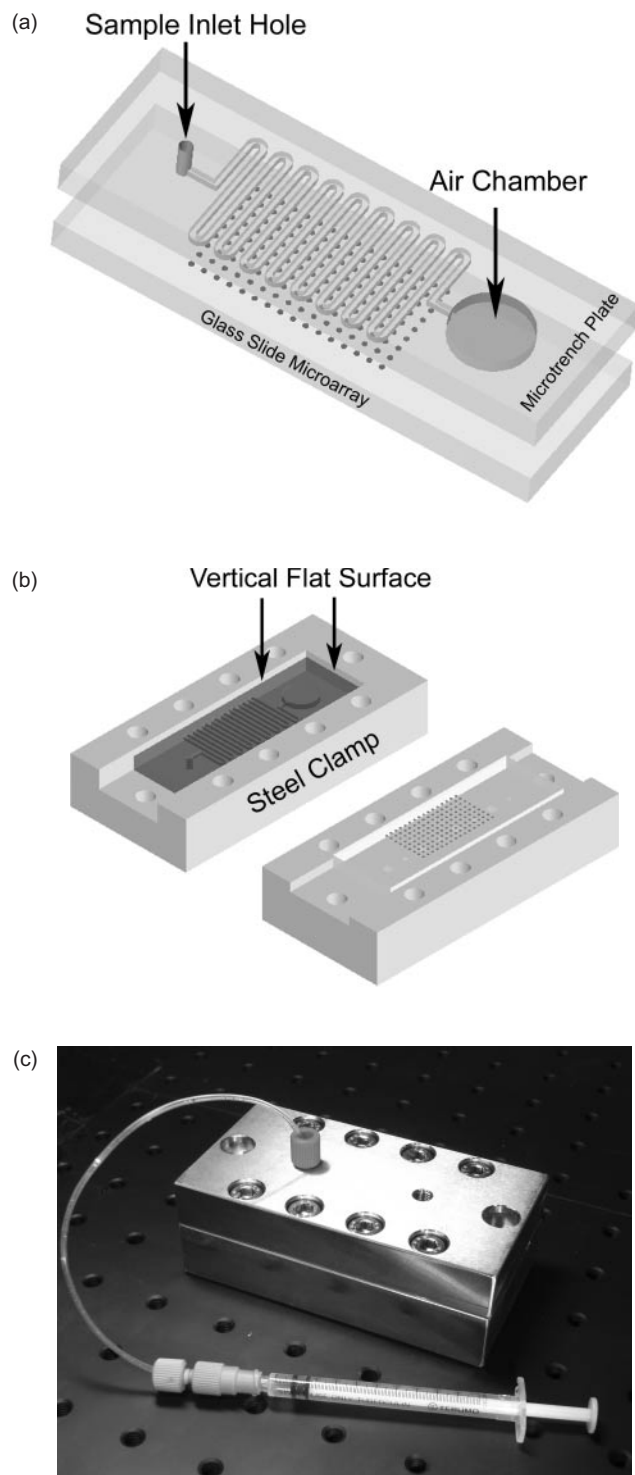
PM: perfect match. MM: mismatch. The 80mer MM sequence is designed to have a 50% GC content but no similarity with the PM sequence. 20mer probes are labeled with NH<sub>2</sub> at the 5'-terminal. The mismatch base is underlined. Targets are labeled with biotin at the 5'-terminal.

sent to the laser scriber for direct machining onto the PMMA substrate. The trench surface was smoothed to have roughness of ~2.4 nm (RMS) according to our previous work (23). The trench width and depth can be varied by changing the laser fabrication parameters. Chips with trenches of depths 50–200 μm are prepared. Normally, a depth of 100 μm is used in hybridization except in studies of the effects of depth, in which 50, 100 and 200 μm are used. The microtrench plate has one opening, a serpentine pattern with 50 straight sections and an air chamber. The overall trench length is 1000 mm. The 50 straight sections encompass 20 mm × 30 mm area. In forming a channel, a PMMA microtrench plate (upper plate in Scheme 2a) is stacked with a conventional glass microarray (lower plate in Scheme 2a). When the two plates are stacked on top of each other, a microarray with microchannels is formed. The microchannel has only a single opening through which to introduce a target solution and to connect to a syringe pump. All reagent solution is introduced and extracted from the opening. The sealed air chamber at the distal terminal of the microchannel is for storing compressed air.

The microtrench is manually aligned with the microarray spots as follows. The distance from one corner of the microarray to the two edges of the slide is set using the arrayer. The same distance is used in fabricating the microtrench chip. The distance from the microtrench to the two edges of the microtrench chip is determined during fabrication using the CO<sub>2</sub> laser scriber. Accordingly, when the edges of the microarray and the microtrench chip are placed against two flat surfaces (the vertical flat surfaces in Scheme 2b), the microarray is automatically aligned with the microtrench. The mechanical alignment procedure is simple and has a spatial repeatability of 10 μm.

### Modifying glass slides

Blank sodalime glass slides are initially sonicated in 1:3 hydrogen peroxide (30%)/sulfuric acid (18 M) solution



**Scheme 2.** (a) A microtrench plate is stacked on a glass microarray slide. (b) Steel clamps (gray cuboids with grooves) for alignment and holding the microtrench/microarray assembly. (c) Photograph of the assembled device with a syringe connected to the inlet hole, sealing the microchannel.

for 1 h at 25°C; rinsed in deionized water (resistivity 18.2 MΩ cm, Millipore) for 5 min, and then sonicated in acetone for 15 min. The slides are then rinsed three times in deionized water for 5 min. They are then dried in a stream of nitrogen; immersed in a solution of 3-(aminopropyl)

triethoxysilane in ethanol (5% v/v) for 1 h; rinsed thoroughly in ethanol and then cured in a vacuum oven at 110°C for 16 h. These home-prepared slides and the commercial aminated slides are then used for spotting DNA probes. Aldehyde-derivatized slides are used to immobilize 20mer 5'-NH<sub>2</sub>-oligonucleotide probes. The aldehyde-derivatized slides are prepared by incubating aminated slides into 10% glutaraldehyde for 1 h. The slides are then rinsed thoroughly in deionized water and dried in a stream of nitrogen.

### Spotting, DNA immobilization and blocking

Oligonucleotide probes are dissolved in 0.1 M 2-(*N*-morpholino)ethanesulfonic acid (MES) solution (24) to a final concentration of 30 μM at pH 6.5. Spotting is performed using a home-built robot equipped with solid pin to deposit probe spots on the glass slide to produce a microarray. The spots have a diameter of ~180 μm. The distance between each pair of spots is 300 μm. The spots are arranged using an arrayer. In the investigation on signal variation, 50 repeated TAL1 probe spots are deposited. Thirty repeated spots are used for 80mer shuttle hybridization and 80mer saturated-target hybridization with flat glass format. For excess-probe hybridization with flat glass format, 300 probes are used. An example showing the arrangement of different probes in the microchannel is in Scheme 1b. For 20mer single base discrimination studies, 25 spots for each probe are used. In all the microarray used in this work, perfect match (PM) and mismatch (MM) probes are deposited on adjacent areas when needed so that the hybridization is performed simultaneously. In the investigation of the limit-of-detection, three repeated spots are deposited. Following spotting, the slides are incubated in a desiccator (~20% relative humidity) at 25°C for 18 h. Ultraviolet irradiation (set to deliver 600 mJ of energy) are then used to crosslink the oligonucleotides of the 80mer oligonucleotide probes onto the slide. For 20mer 5'-NH<sub>2</sub>-oligonucleotide probes, slides are washed once with 0.1% SDS, twice with deionized water, and then incubated for 5 min with sodium borohydride (NaBH<sub>4</sub>) solution (in which 2.5 mg of NaBH<sub>4</sub> is dissolved in 750 μl of PBS and 250 μl of 100% ethanol); they are then incubated for 3 min with deionized water. After integration with the microchannel chip, the array is then blocked using 5× SSC, 0.1% SDS and 0.1% BSA at 42°C for 30 min, and rinsed three times in deionized water for 5 min before hybridization.

### Shuttle hybridization and static microchannel hybridization

For 80mer hybridization, Biotin-labeled target ssDNA is diluted in 50% formamide, 5× SSC and 0.1% SDS, to a final concentration from 0.02 pM to 90 nM. For 20mer single base discrimination studies, the target concentration is 90 nM. For shuttle hybridization, 1 μl DNA target solution is introduced into the microchannel opening shown in Scheme 2a using a pipette. A syringe is then connected to the opening, sealing the microchannel. The sample solution is pushed to the distal side of the channel, away from the opening, when the syringe is compressed. The distal terminal of the channel is sealed and the compressed air is stored in the distal chamber. Hence the sample solution bounces back when the compressed syringe is released. In shuttle hybridization, the target solution is mixed with the probes while being pumped back and forth inside the

entire channel, sweeping over the probes. The cycle time of the shuttling is 2 s. In static microchannel hybridization, the sample is introduced into the microchannel according to the same scheme but no shuttling is applied. The entire microarray/microchannel assembly is placed in a 42°C water bath to control the temperature. Following hybridization, the target solution is drawn from the channel and discarded. Several buffer solutions are introduced into, and then drawn out, to perform washing: 10  $\mu$ l of 2 $\times$  SSC, 0.1% SDS at 42°C, 20  $\mu$ l 0.1 $\times$  SSC, 0.1% SDS at 25°C and 20  $\mu$ l 0.1 $\times$  SSC at 25°C are used. Each wash takes 5 min. The array is then incubated with 1  $\mu$ l Cy5-conjugated Streptavidin (SA-Cy5, 0.05 mg/ml) (Zymed, CA) with reagent shuttling for 5 min at 25°C, followed by washing in 2 $\times$  SSPE/0.1% SDS. The microarray is then detached from the microtrench plate to be scanned to detect fluorescence signals. After hybridization and SA-Cy5 staining, the microtrench only shows fluorescence of background level comparable to that of the microarray background.

### Conventional flat glass hybridization

Conventional flat glass hybridization is conducted as follows. A Gene Frame (Abgene, UK) is attached to the microarray slide to produce a sealed chamber. A 300  $\mu$ l target DNA is used in saturated target hybridization. In excess-probe experiment, 300 repeated TAL1 probe spots are hybridized with 30  $\mu$ l target DNA. The temperature of hybridization is 42°C, and the slide is incubated in a humidified chamber. Following hybridization, the slides are washed in 2 $\times$  SSC, 0.1% SDS at 42°C for 5 min, 0.1 $\times$  SSC, 0.1% SDS at 25°C for 10 min and 0.1 $\times$  SSC at 25°C for 5 min. The flat glass array is then incubated with 40  $\mu$ l SA-Cy5 at 25°C for 60 min, and then washed with 2 $\times$  SSPE/0.1% SDS. For 20mer single base discrimination studies, the target concentration is 90 nM and the volume is 25  $\mu$ l.

### Quantifying fluorescence image

Following hybridization and SA-Cy5 incubation, the microarray slides are scanned at a resolution of 5  $\mu$ m using a GenePix 4000B array scanner (Axon Instrument, CA). The PMT voltage is set to 700 V. The hybridization signal from multiple copies of probes is averaged and used in analyzing the data.

## RESULTS AND DISCUSSION

### Typical microtrench structure

The SEM image in Figure 1 presents a typical structure of the microtrench in a PMMA chip used for shuttle hybridization. In this image, the width and depth of the straight sections of the microtrench are 200 and 100  $\mu$ m, respectively. The length of the straight sections is 18 mm. The entire chip has 50 straight sections connected with U-turns. The depth at the turn is intentionally increased to 300  $\mu$ m. The distance between the straight sections is 300  $\mu$ m. The channel width, depth and length, and the distance between adjacent sections are varied according to the layout of the microarray. The chip is to be stacked with a flat glass DNA microarray. The device is compatible with the normal DNA microarray format. The microtrench is then sealed with the flat glass by tightening the screws on the clamp (Scheme 2), forming a microchannel with alternating cross-sections at successive turns. The alternating cross-section produces turbulence at the turns. When a continuous

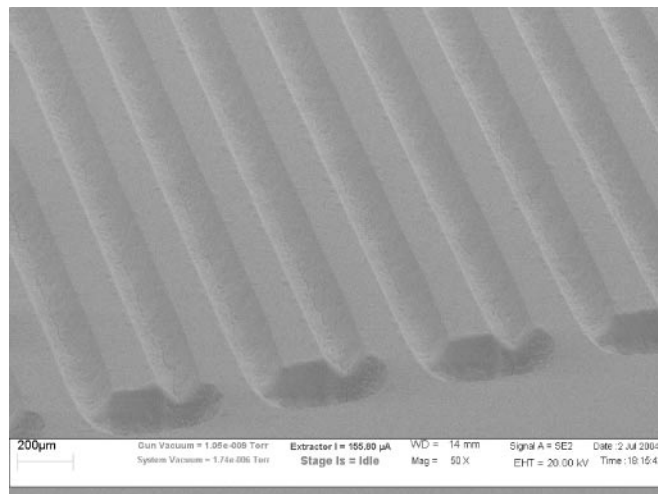


**Figure 1.** Typical structure of the microtrench used in the shuttle hybridization device. The trench width is 200  $\mu$ m and the depth is 100  $\mu$ m at the straight sections. The depth at the turns in this example is 300  $\mu$ m.

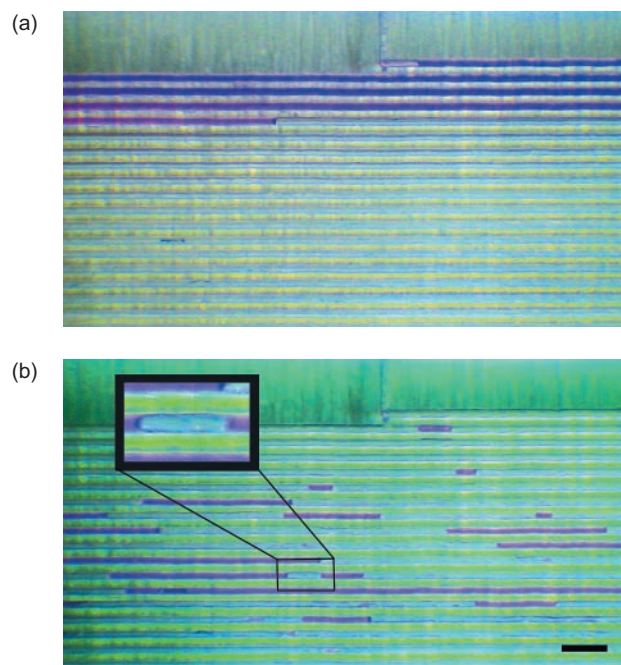


**Figure 2.** Microscopic images of the liquid plugs. (a) A long 2  $\mu$ l continuous glycerol plug with clear blue and red sections that are not well mixed. Printer inks are dissolved in glycerol in the two sections. (b) The scrambled discrete plugs resulted from shuttling the plug in (a) back and forth once in the microchannel. The scale bar is 1 mm. Discrete plugs are produced when the solution is pumped back and forth through the serpentine channel. Thorough mixing is obtained, as shown by the homogeneous purple plugs. The inset shows liquid meniscus at the plug/air interface.

sample (Figure 2a) is transported through these turns, it is randomly scrambled into discrete short plugs, as shown in Figure 2b. Figure 2b reveals that the lengths of these plugs range from several hundred micrometers to several millimeters, as observed under a microscope. The re-circulation flow inside such plugs has been described in various studies (18,21). These liquid plugs are separated by air and span

a length of  $\sim 100$   $\mu\text{m}$  in the microchannel. When transported to the two termini of the microchannel, the plugs combine to form one big plug because of the surface tension of the aqueous solution, as observed by a video microscope (data not shown). During the hybridization or the SA-Cy5 incubation, each discrete plug is allowed to sweep over all of the probes in the microchannel when it is transported back and forth between the termini. In this way, the reagent sample is allowed to react with all the probes deposited in the entire array without filling the entire channel simultaneously. The relatively rigid PMMA is used as the microchannel chip, and the high dimensional stability simplifies the alignment procedure. This simplification is a great advantage over the procedure that involves an elastic PDMS substrate, which is also extensively used in microfluidic chip investigations.

### Expedited hybridization equilibrium in the shuttle hybridization

No clear difference between the home-prepared slides and the commercial slides on the hybridization signal was found. Therefore, this work does not compare their performance.

The shuttle hybridization signal reaches equilibrium very rapidly. Figure 3a plots the signal rise for various hybridization formats. As the signal associated with the excess-probe and saturated-target flat glass hybridizations continue to grow beyond 4 h, the signal for shuttle hybridization reaches 95% of the final intensity in  $<10$  min. Notably, the same target concentration is used for all three formats. The final intensity is higher in the saturated-target flat glass hybridization because the target quantity used in the flat glass format is 300 times larger than in shuttle hybridization. It is also observed that in the saturated-target experiment the signal increases faster than the excess-probe experiment. This suggests that different targets that have different quantities in a sample solution do not hybridize at the same rate.

Figure 3b presents the details of the signal growth for a short hybridization time. Also shown in Figure 3b is the run-to-run reproducibility of the shuttle hybridization. The fluorescence signal from two repeated experiments, Shuttle 1 and Shuttle 2 do not show significant difference. One-way ANOVA (analysis of variance) was also used to compare the result from three repeated experiments. No significant difference was found ( $P=0.814-0.843 > 0.05$ , the significance level).

The signal associated with shuttle hybridization reaches equilibrium more rapidly than the other formats do. The signal for the flat glass hybridization increases with the hybridization time between 125 and 1000 s and is faster than the static microchannel hybridization. The diagonal length of a 20 mm  $\times$  30 mm flat glass microarray is 36 mm. When the relatively small diffusion constant is considered, the fact that the kinetics are controlled by diffusion is unsurprising. However, to the authors' surprise, the growth of the signal is even slower for the static microchannel hybridization than for the saturated-target flat glass format. This phenomenon can be understood by the fact that the available complementary target molecules are fewer for the probes in a static microchannel than in the saturated-target flat glass format. When the nearby target is depleted by hybridizing to the probes in the static microchannel, more targets must be supplied by diffusion along the channel. The width (200  $\mu\text{m}$ ) of the channel is

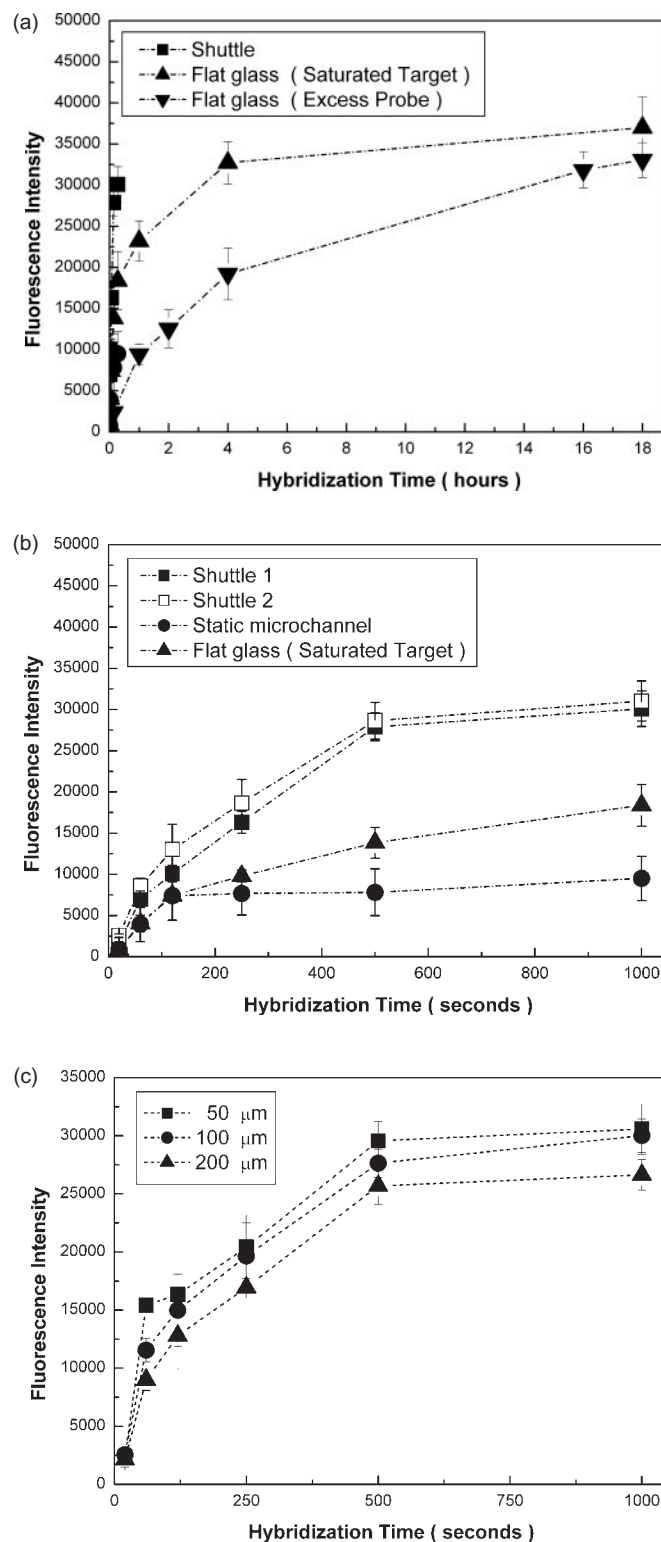


**Figure 3.** Hybridization signal growth for various formats, shuttle hybridization (squares), flat glass hybridization (triangles) and static microchannel hybridization (circles) for a hybridization time of up to 18 h (a) and 1000 s (b). Shuttle 1 and Shuttle 2 in (b) are repeated experiments. The target concentration is 90 nM. For saturated-target hybridization, 300  $\mu\text{l}$  target is hybridized to 30 probe spots. For excess-probe hybridization, 30  $\mu\text{l}$  target is hybridized to 300 probe spots. (c) Hybridization signal growth for shuttle hybridization at various channel depths (squares, 50  $\mu\text{m}$ ; circles, 100  $\mu\text{m}$ ; and triangles, 200  $\mu\text{m}$ ).

three orders shorter than the overall channel length (1000 mm), so the diffusion process can be considered to be one-dimensional like. These limitations relate to the slow kinetics observed for the static microchannel. Additionally, the slow kinetics reveals that the expedited equilibrium in shuttle hybridization is not caused by the reduced diffusion length between the probes and targets inside the microchannel.

A further experiment supports this claim. Figure 3c presents the signal growth in shuttle hybridization with various channel depths. The finding reveals that the signals all reach equilibrium after  $\sim 500$  s of hybridization, independent of the channel depth. The small channel dimensions do not explain the short time required to reach equilibrium.

The target used in the hybridization study described above is 80mer synthetic oligonucleotide with 5'-terminal singly labeled biotin. The molecular weight of biotin is 244. It is relatively small compared to the oligonucleotide molecule and is considered not to affect the diffusion constant of the oligonucleotide. The corresponding diffusion constant of 80mer oligonucleotide in water is  $D_w = 2.1 \times 10^{-7} \text{ cm}^2/\text{s}$  (6). A reaction time of 18 h (64 800 s) corresponds to a diffusion length of  $\sim 1.6$  mm for the 80mer DNA. The viscosity of the hybridization solution is normally higher than that of water. Therefore, a lower diffusion length is expected in hybridization buffer. The microfluidic droplet chaotic mixing used herein reduced the mixing time by two orders of magnitude (64 800 s / 500 s) below that obtained using conventional flat glass hybridization. This enhancement is very large. The following further examination is conducted to verify the reason for the enhancement.

Song *et al.* (21) showed that for constant channel dimension and plug flow velocity, the droplet flow chaotic mixing time is proportional to  $\log(1/D)$ , where  $D$  is the diffusion constant. For instance, the mixing time for a channel width of  $100 \mu\text{m}$ , a flow of  $18 \text{ mm/s}$  and a diffusion constant of  $2 \times 10^{-6} \text{ cm}^2/\text{s}$  is  $\sim 65$  ms, whereas the time required for pure diffusion is  $\sim 50$  s (21). The enhancement is about three orders of magnitude. This example reveals that the mixing inside the droplet is almost instantaneous, as the sample sweeps over each DNA probe in the microchannel. Since the mixing is instantaneous whereas the hybridization takes  $\sim 500$  s, it is obvious that some other effects may impede the hybridization so that the hybridization does not reach equilibrium when mixing is complete.

In the shuttle hybridization, the sample is separated into small discrete plugs. Assuming instantaneous and complete mixing among all separate plugs, as observed in Figure 2a and b, the hybridization signal should reach ultimate equilibrium for a single sample pass when all targets are mixed thoroughly with the probes. However, the hybridization equilibrium is observed after  $\sim 500$  s. This fact reveals that multiple passes are required to enable the current device to reach hybridization equilibrium, and suggests that the DNA pairing reaction may be the limiting step in the shuttle hybridization format. The surface electrostatic effect and steric interactions may critically determine the hybridization kinetics (25). This finding may also indicate that global mixing in the current device is inefficient. Further work is in progress to study the hybridization efficiency of long target DNA in order to clarify other possible effects.

Another benefit of the chaotic mixing of the droplets is the reduced effect of the diffusion constant on the mixing time.

When combined with the equation for the diffusion constant of DNA in water,  $D_w = 4.9 \times 10^{-9} \times [\text{bp}]^{-0.72}$ , the droplet chaotic mixing time is  $T = 0.72 \log[\text{bp}]$ . Restated, the mixing time for 800 bp DNA is only 1.5 times longer than that of 80mer DNA. The use of long target DNA is thus expected to extend the required hybridization time only slightly.

### Quality of data concerning shuttle hybridization

As well as the fast reaching of hybridization equilibrium, shuttle hybridization also involves signals of better quality than those yielded by flat glass hybridization. The signal variation, the S/N ratio and the hybridization specificity are carefully investigated as follows.

Fifty TAL1 probe spots are equally distributed over the 50 straight sections in the microchannel to determine whether  $1 \mu\text{l}$  sample can hybridize all of the probes in the microarray. One probe spot is deposited in each straight section to span the 50 spots over the entire microchannel. Five thousand probe spots with an inter-spot distance of  $200 \mu\text{m}$  can be deposited in the entire channel. A  $1 \mu\text{l}$  target solution can hybridize in the microchannel. Figure 4 shows a histogram of the resultant fluorescence signal distribution. The signal variation associated with the 50 spots is 5.2% (CV). For comparison, the signal variation associated with flat glass hybridization, which involves pure diffusion, is  $\sim 25\%$  (10,26). The results herein reveal that  $1 \mu\text{l}$  target solution suffices for a 5000-probe microarray. Moreover, the distance from the first to the fiftieth straight section is  $\sim 1$  m. The result demonstrates that the shuttle hybridization offers uniform hybridization efficiency when a small volume is passed through the long channel, as shown in the inset in Figure 4. No difference between the sections near the sample inlet hole and those near the distal air chamber is observed. Notably,  $1 \text{ fmol}$  ( $1 \mu\text{l} \times 1 \text{ nM}$ ) of the target was used in this experiment. With fifty repeated probe

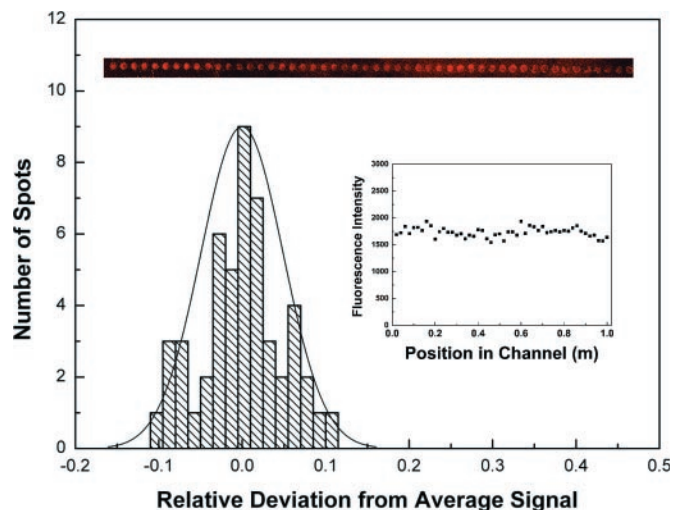


**Figure 4.** Signal variation across the entire microarray in shuttle hybridization is investigated using a histogram of the hybridization signal from 50 identical probe spots evenly distributed over the entire microchannel. The overall channel length is 1 m. The 50 spots are deposited in the 50 straight sections in the channel. The solid line is a Gaussian fit. The target concentration is 1 nM and the hybridization time is 500 s. The sample volume is  $1 \mu\text{l}$ . The inset presents the fluorescence image of the 50 spots and their corresponding intensities at various locations in the channel.

spots in the array, this number, 1 fmol, is very close to the detection limit (19 pM, see below). More probe spots must consume more target to give a similar signal intensity (27). The observation is consistent with the literature. Shuttle hybridization has a lower signal variation than flat glass hybridization. Importantly, 5000 spots are not the limit for the 1  $\mu$ l sample. This number was used as an example and the upper limit has not yet been confirmed.

The shuttle hybridization not only provides a reduced equilibrium time, consumes less reagent, and lower signal variation; its S/N ratio is also greater. Figure 5 presents the fluorescence images and the S/N ratio of the perfect match probes (80 PM) and the non-complementary probes (80 MM) hybridized with a perfect match target. The corresponding fluorescence images for various hybridization formats at 500 s and a hybridization time of 18 h are also presented. The shuttle hybridization at 500 s reveals a highest S/N ratio that is  $\sim 2.2$  times higher than that obtained by flat glass hybridization time after 18 h. High S/N ratio is obtained along with the fast kinetics for the shuttle hybridization. Moreover, whether the reduction in the background contributes to the increase in the S/N ratio remains of interest.

During flat glass hybridization, trapped air bubbles severely stain the fluorescence image and substantially increase the background. The discrete plugs in the shuttle hybridization are separated by air, so whether the air inside the microchannel increases the background is of interest. The background in the shuttle hybridization is slightly lower than that in the flat glass hybridization (data not shown). The authors posit that this

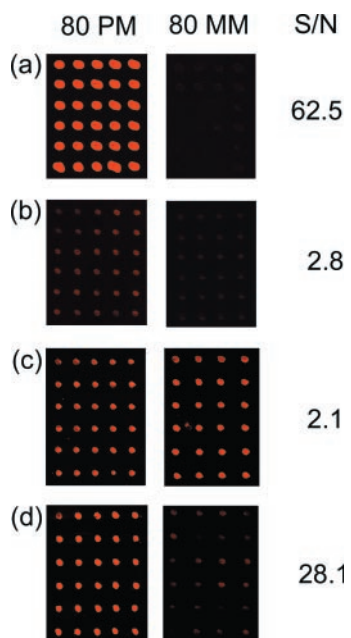


**Figure 5.** S/N ratios for various hybridization formats: (a) shuttle hybridization at 500 s; (b) static microfluidic hybridization at 500 s; (c) flat glass hybridization at 500 s; and (d) flat glass hybridization at 18 h. The target concentration is 90 nM. The sample volumes are 30  $\mu$ l, 10  $\mu$ l and 1  $\mu$ l for the three formats—flat glass hybridization, static microfluidic and shuttle hybridization, respectively. The total probe spot is 30 for (a) and (b) and 300 for (c) and (d). The left column presents the fluorescence images with PM (80 PM) probe, and the right column presents the fluorescence images with MM (80 MM) probe.

difference follows from the following reasons. The volume in the microchannel is small, being 10–20  $\mu$ l for the whole channel. The air inside the microchannel is therefore full of moisture from the nearby aqueous solution. The air is not dry, hence no precipitation occurs from adjacent liquid plugs so that the air plug causes no staining. Channel wall covered with residual film of water also could suppress the drying of the surface. Shuttle hybridization is thus concluded to slightly reduce the background, potentially reducing the detection limit.

In conventional hybridization assays, the specificity hybridization is achieved by adjusting the hybridization conditions or the washing conditions of the probe–target duplex. In DNA microarray assays, however, this method cannot be easily applied because one set of hybridization and washing conditions does not optimally distinguish among all probes on the microarray. Shuttle hybridization via mixing increases hybridization specificity. Figure 6 presents the S/N ratio of the single-base-pair-mismatch hybridization of various 20mer oligonucleotide probes and displays the corresponding fluorescence images for various hybridization formats. Except when the MM1 probe is used, the S/N ratios from the shuttle hybridization all exceed 3, indicating good discrimination. The reason for the poor discrimination of MM1 is beyond the scope of this investigation, although the strong steric hindrance near the surface of the slide is posited as the cause. The effect of steric hindrance and the extent of the impact on the stability of the duplex due to various mismatch pairs (28,29)

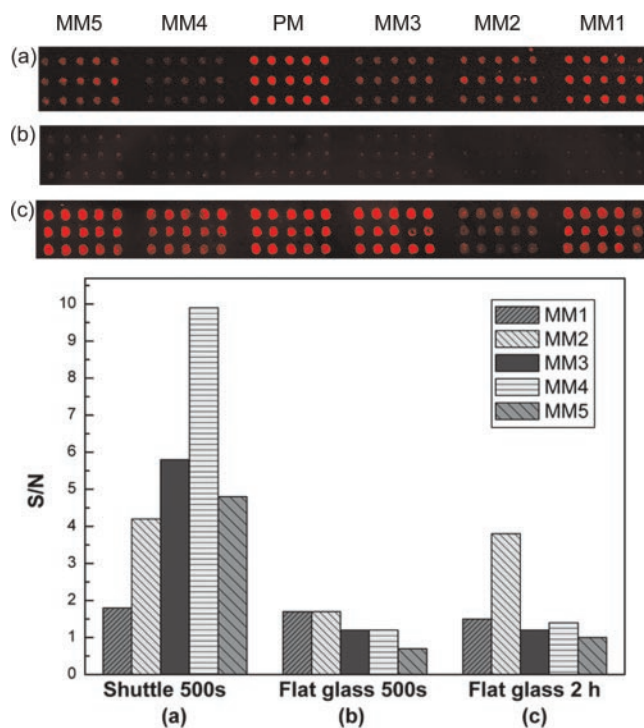


**Figure 6.** S/N ratio of single-base-pair-mismatch hybridization for 20mer oligonucleotide probes and corresponding fluorescence images for various hybridization formats. (a) Shuttle hybridization after 500 s; (b) flat glass hybridization after 500 s; and (c) flat glass hybridization after 2 h. The target concentration is 90 nM and the volume is 1  $\mu$ l for shuttle hybridization and 25  $\mu$ l for flat glass hybridization, respectively. The number of spot for each probe is 25.



explain the discrimination difference of different PM-MM pairs. Shuttle hybridization effectively discriminates single base mismatch, but no discrimination is observed after 500 s of flat glass hybridization. When the hybridization time is increased to 2 h, only one of the five mismatch probes exhibits a discrimination of S/N ratio greater than three. These data show that the mixing effect of the plug flow improves the specificity of hybridization.

**Reduced sample consumption in shuttle hybridization**

The detection limit of this new hybridization format was determined. The signal to background ratio (S/B) was measured as the target was diluted. As shown in Figure 7, the detection limit at S/B = 3 is 19 pM (19 amol in 1 μl). The finding herein shows the good performance of the shuttle hybridization, in relation to the 12 pM detection limit associated with special substrate surface (12). Notably, the widely available microarray slide is used in this work. A 1 μl target sample was used and 19 amol was determined as the molar detection limit. This value corresponds to  $1.1 \times 10^7$  singly labeled copies per transcript in the sample. The low detection limit was obtained when the ordinary glass slide was used because in the shuttle hybridization, the mixing is between the probes and all the targets in the sample solution and is not only between those within the diffusion length. The shuttling strategy efficiently brings all target molecules in contact with all probes in the microarray. The strategy greatly increases the hybridization efficiency in a simple manner. A multiply labeled target could be used to reduce the detection limit further.

For average target labeling in the cDNA microarray experiment, the optimal fluorophore labeling density is 1 fluorophore/20–25 nt (30). A labeled cDNA target obtained by oligo-dT primed reverse-transcription normally has a length from ~300 bp to several kilo base pairs (8,31). Based on the assumption that the cDNA molecule has an average length of ~1000 bp, the expected detection limit obtained using shuttle

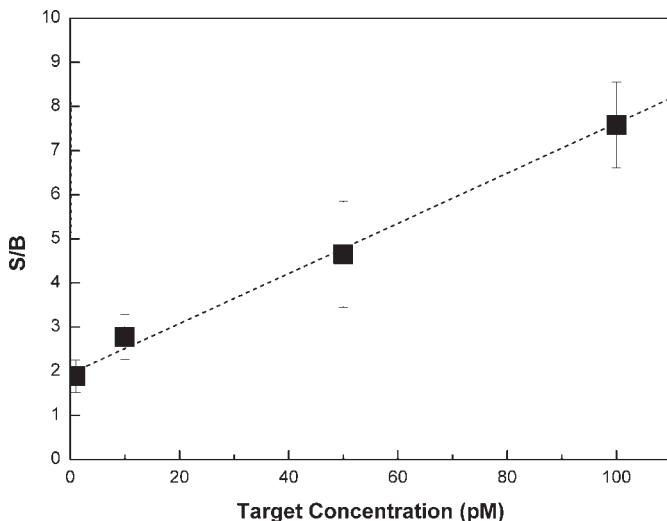


**Figure 7.** Fluorescence S/B ratio for shuttle hybridization as a function of the target concentration. The dashed line is a linear fit.

hybridization can be reduced to 1/50 of the current value. This value corresponds to  $2 \times 10^5$  copies per transcript in the sample. Restated, only  $2 \times 10^5$  cells are required to enable single-copy genes to be detected using shuttle hybridization. A further experiment on the analysis of gene expression is in progress to test this inference.

Systematic bias is known to occur in hybridization that does not reach equilibrium (4), because a low-copy target reaches equilibrium more slowly than the high-copy targets do. The incomplete hybridization therefore results in the over-estimation of the expression of the up-regulated genes and the underestimation of the expression of the down-regulated genes. Whether the shuttle hybridization reduced the systematic bias was tested. Figure 8 plots the increase in intensity with increased hybridization time at various target concentration. At tested concentrations from 50 pM to 90 nM for the shuttle hybridization (Figure 8a), the equilibrium time was the same, at ~500 s. On the contrary, for flat glass hybridization (Figure 8b), higher target concentration reaches hybridization equilibrium faster. This finding demonstrates that the shuttle hybridization drives the reaction to equilibrium with a time

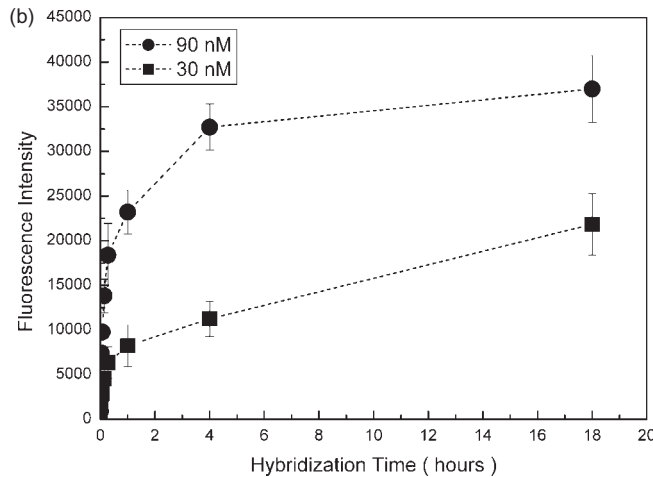
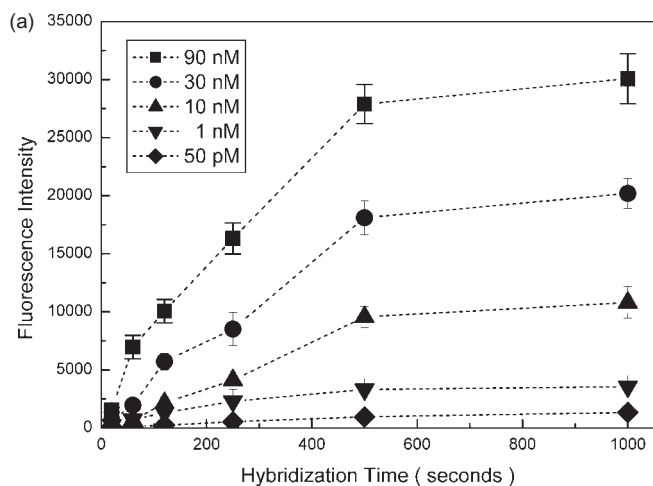


**Figure 8.** (a) Hybridization signal growth of 80mer TAL1 target at various target concentrations in shuttle hybridization, showing reduced concentration bias. The target volume is 1 μl and the number of probe spot is 30. (b) Flat glass hybridization equilibrium at different target concentration.

independent of the target concentration. This characteristic helps to reduce the systematic bias associated with flat glass hybridization. A single target molecule is used herein, so influence on the hybridization rate by sequence variation does not play a role. Another experiment is being performed, using a multiply labeled target to test the equilibrium time at lower concentration.

## CONCLUSION

Discrete sample plugs were used in DNA microchannel hybridization to take advantage of the chaotic mixing of droplets. A 1  $\mu$ l target was used for hybridization with an array that can hold 5000 probes. The shuttle hybridization method resulted in the fast reaching of equilibrium when the 80mer target DNA was used. A hybridization time of 500 s sufficed to drive the reaction to equilibrium. The detection limit was 19 amol ( $1.1 \times 10^7$  molecules) when the singly labeled target was used. An ordinary flat glass microarray was used in the shuttle hybridization and a common fluorescence scanner was used to detect the fluorescence. The method is completely compatible with the extensively used flat glass DNA microarray format. The quality of the data on the S/N ratio, the signal variation, the background growth and the single base discrimination were investigated carefully. Rigid PMMA was used as the microfluidic chip substrate to facilitate manual alignment between the microfluidic chip and the microarray chip. A further study, using the shuttle hybridization method for gene expression is under way. In particular, a DNA target with multiple fluorescence labeling is being tested to reduce the detection limit.

## ACKNOWLEDGEMENTS

We would like to thank Prof. Hsueh-Chia Chang, University of Notre Dame, USA and Prof. Shau-Chun Paul Wang, National Chung Cheng University, Taiwan, for their valuable discussion on this study. We thank Academia Sinica, Taiwan and the National Science Council, Taiwan for their financial support. Funding to pay the Open Access publication charges for this article was provided by Academia Sinica, Taiwan.

*Conflict of interest statement.* None declared.

## REFERENCES

- Wang, H.Y., Malek, R.L., Kwitek, A.E., Greene, A.S., Luu, T.V., Behbahani, B., Frank, B., Quackenbush, J. and Lee, N.H. (2003) Assessing unmodified 70-mer oligonucleotide probe performance on glass-slide microarrays. *Genome Biol.*, **4**, R5.
- Stillman, B.A. and Tonkinson, J.L. (2001) Expression microarray hybridization kinetics depend on length of the immobilized DNA but are independent of immobilization substrate. *Anal. Biochem.*, **295**, 149–157.
- Sterrenburg, E., Turk, R., Boer, J.M., van Ommen, G.B. and den Dunnen, J.T. (2002) A common reference for cDNA microarray hybridizations. *Nucleic Acids Res.*, **30**, e116.
- Bhanot, G., Louzoun, Y., Zhu, J.H. and DeLisi, C. (2003) The importance of thermodynamic equilibrium for high throughput gene expression arrays. *Biophys. J.*, **84**, 124–135.
- Sartor, M., Schwanekamp, J., Halbleib, D., Mohamed, I., Karyala, S., Medvedovic, M. and Tomlinson, C.R. (2004) Microarray results improve significantly as hybridization approaches equilibrium. *Biotechniques*, **36**, 790–796.
- Lukacs, G.L., Haggie, P., Seksek, O., Lechardeur, D., Freedman, N. and Verkman, A.S. (2000) Size-dependent DNA mobility in cytoplasm and nucleus. *J. Biol. Chem.*, **275**, 1625–1629.
- Bard, A.J. and Larry, R.F. (1980) *Electrochemical Methods—Fundamental and Applications*. John Wiley & Sons Inc., New York.
- Whitney, A.R., Diehn, M., Popper, S.J., Alizadeh, A.A., Boldrick, J.C., Relman, D.A. and Brown, P.O. (2003) Individuality and variation in gene expression patterns in human blood. *Proc. Natl Acad. Sci. USA*, **100**, 1896–1901.
- Wang, J., Robinson, J.F., Khan, H.M., Carter, D.E., McKinney, J., Miskie, B.A. and Hegele, R.A. (2004) Optimizing RNA extraction yield from whole blood for microarray gene expression analysis. *Clin. Biochem.*, **37**, 741–744.
- Cheek, B.J., Steel, A.B., Torres, M.P., Yu, Y.Y. and Yang, H. (2001) Chemiluminescence detection for hybridization assays on the flow-thru chip, a three-dimensional microchannel biochip. *Anal. Chem.*, **73**, 5777–5783.
- Adey, N.B., Lei, M., Howard, M.T., Jensen, J.D., Mayo, D.A., Butel, D.L., Coffin, S.C., Moyer, T.C., Slade, D.E., Spute, M.K. *et al.* (2002) Gains in sensitivity with a device that mixes microarray hybridization solution in a 25- $\mu$ m-thick chamber. *Anal. Chem.*, **74**, 6413–6417.
- Liu, Y.J. and Rauch, C.B. (2003) DNA probe attachment on plastic surfaces and microfluidic hybridization array channel devices with sample oscillation. *Anal. Biochem.*, **317**, 76–84.
- Wang, Y., Vaidya, B., Farquar, H.D., Stryjewski, W., Hammer, R.P., McCarley, R.L., Soper, S.A., Cheng, Y.W. and Barany, F. (2003) Microarrays assembled in microfluidic chips fabricated from poly(methyl methacrylate) for the detection of low-abundant DNA mutations. *Anal. Chem.*, **75**, 1130–1140.
- Cheng, J.-Y., Wei, C.-W., Hsu, K.-H. and Young, T.-H. (2002) In Baba, Y., Shoji, S. and Berg, A.v.d. (eds), *Micro Total Analysis Systems 2002*. Kluwer, Nara, Japan, Vol. 1, pp. 458–460.
- Erickson, D., Li, D.Q. and Krull, U.J. (2003) Modeling of DNA hybridization kinetics for spatially resolved biochips. *Anal. Biochem.*, **317**, 186–200.
- Yaralioglu, G.G., Wygant, I.O., Marentis, T.C. and Khuri-Yakub, B.T. (2004) Ultrasonic mixing in microfluidic channels using integrated transducers. *Anal. Chem.*, **76**, 3694–3698.
- Stroock, A.D., Dertinger, S.K., Ajdari, A., Mezic, I., Stone, H.A. and Whitesides, G.M. (2002) Chaotic mixer for microchannels. *Science*, **295**, 647–651.
- Tice, J.D., Lyon, A.D. and Ismagilov, R.F. (2004) Effects of viscosity on droplet formation and mixing in microfluidic channels. *Anal. Chim. Acta*, **507**, 73–77.
- Ottino, J.M. (1989) *The Kinematics of Mixing: Stretching, Chaos, and Transport*. Cambridge University, Cambridge.
- Tice, J.D., Song, H., Lyon, A.D. and Ismagilov, R.F. (2003) Formation of droplets and mixing in multiphase microfluidics at low values of the Reynolds and the capillary numbers. *Langmuir*, **19**, 9127–9133.
- Song, H., Bringer, M.R., Tice, J.D., Gerds, C.J. and Ismagilov, R.F. (2003) Experimental test of scaling of mixing by chaotic advection in droplets moving through microfluidic channels. *Appl. Phys. Lett.*, **83**, 4664–4666.
- Song, H., Tice, J.D. and Ismagilov, R.F. (2003) A microfluidic system for controlling reaction networks in time. *Angew. Chem.-Int. Edit.*, **42**, 768–772.
- Cheng, J.-Y., Wei, C.-W., Hsu, K.-H. and Young, T.-H. (2004) Direct-write laser micromachining and universal surface modification of PMMA for device development. *Sens. Actuator B-Chem.*, **99**, 186–196.
- Zammatteo, N., Jeanmart, L., Hamels, S., Courtois, S., Louette, P., Hevesi, L. and Remacle, J. (2000) Comparison between different strategies of covalent attachment of DNA to glass surfaces to build DNA microarrays. *Anal. Biochem.*, **280**, 143–150.
- Peterson, A.W., Heaton, R.J. and Georgiadis, R.M. (2001) The effect of surface probe density on DNA hybridization. *Nucleic Acids Res.*, **29**, 5163–5168.
- Fixe, F., Dufva, M., Telleman, P. and Christensen, C.B.V. (2004) Functionalization of poly(methyl methacrylate) (PMMA) as a substrate for DNA microarrays. *Nucleic Acids Res.*, **32**, e9.
- Franssen-van Hal, N.L., Vorst, O., Kramer, E., Hall, R.D. and Keijer, J. (2002) Factors influencing cDNA microarray hybridization on silylated glass slides. *Anal. Biochem.*, **308**, 5–17.

28. Aboul-ela, F., Koh, D., Tinoco, I., Jr and Martin, F.H. (1985) Base-base mismatches. Thermodynamics of double helix formation for dCA3XA3G + dCT3YT3G (X, Y = A, C, G, T). *Nucleic Acids Res.*, **13**, 4811–4824.
29. Ikuta, S., Takagi, K., Wallace, R.B. and Itakura, K. (1987) Dissociation kinetics of 19 base paired oligonucleotide–DNA duplexes containing different single mismatched base-pairs. *Nucleic Acids Res.*, **15**, 797–811.
30. 't Hoen, P.A., de Kort, F., van Ommen, G.J.B. and den Dunnen, J.T. (2003) Fluorescent labelling of cRNA for microarray applications. *Nucleic Acids Res.*, **31**, e20.
31. Tsai, C.C., Chung, Y.D., Lee, H.J., Chang, W.H., Suzuki, Y., Sugano, S. and Lin, J.Y. (2003) Large-scale sequencing analysis of the full-length cDNA library of human hepatocellular carcinoma. *J. Biomed. Sci.*, **10**, 636–643.